

Impulse response estimation method for ultrasound arrays

Pim van der Meulen*, Pieter Kruizinga*[†], Johannes G Bosch[†], Geert Leus*

*Delft University of Technology, Delft, The Netherlands

[†]Erasmus Medical Center, Rotterdam, The Netherlands

Abstract—We present a method for estimating the one-way electro-mechanical impulse response or transfer function of self-reciprocal ultrasound transducers. The one-way impulse response is needed for forward field simulations, or for pulse-echo simulations and excitation code design when the one-way impulse response per array element is different. Using a flat plate reflector that is positioned parallel to the transducer surface, the resulting pulse-echo signal is measured. Since the transducer is self-reciprocal, the transmit and receive impulse responses are equivalent. Consequently, the measured signal is the autoconvolution of the one-way impulse response. We propose a new de-autoconvolution algorithm to obtain the one-way impulse response from such a signal. The proposed measurement procedure is especially time-efficient for large arrays, and does not rely on hydrophones or additional transducers. Experimental results are shown to demonstrate the effectiveness of the proposed method.

I. INTRODUCTION

Accurate knowledge of the one-way electro-mechanical impulse response or transfer function is important for e.g. model-driven beamforming techniques and accurate ultrasound simulations. Typical transducer calibration procedures (e.g. [1], [2]) result in an estimate of the *pulse-echo* impulse response, which are only useful for pulse-echo simulations: they estimate the combined effect of the transmit and receive impulse responses. For computing the forward field, however, the *one-way* impulse response is of interest. Another example is that of an array transducer where each element may have a somewhat different impulse response, e.g. due to imprecisions in the transducer production process. As a result, the pulse-echo impulse response from one array element to another may be different for each combination of elements. In this case, it is convenient to know the pulse-echo response for each combination of transmit and receive elements for either simulations, model-based imaging, or excitation code design.

Even if one is only interested in the pulse-echo transfer function, measuring the pulse-echo impulse response for each combination of transmit and receive elements is a very laborious process for large arrays. In that case, it would be more convenient to use a hydrophone to measure the transmitted pulse of each transducer excited by a delta-pulse. The pulse-echo impulse response between transmit/receive pairs is then found by convolving the corresponding impulse responses. However, hydrophone setups are expensive, the procedure is time-consuming, and the measurement is sensitive to the hydrophone position relative to the transducer. Our proposed method does not rely on hydrophone measurements, but uses the pulse-echo measurement of the reflection from

a flat reflector. An additional benefit of this method over the hydrophone-based characterization is that the signal to noise ratio (SNR) of the pulse-echo measurements may be much better if the transducer under test has a large measurement surface compared to the hydrophone surface. Moreover, the transducer is more likely to have a high sensitivity in its own bandwidth compared to hydrophones, resulting in increased SNR.

Many other characterization procedures exist to determine the one-way impulse response, but require experimental setups that directly measure the transducer input and output voltage and currents (see e.g. [3–7]). This type of method typically requires some knowledge of the incident or transmitted pressure field, hence involving additional transducers, which need to be carefully aligned for each measurement in an array. Alternatively, they assume a specific type of wave is transmitted to avoid using additional transducers.

Here we present a simple procedure to estimate the one-way impulse response using only one digitized pulse-echo measurement per array element by means of a new de-autoconvolution algorithm, not involving hydrophones. If the transducer under test is self-reciprocal, the transmit and receive impulse responses are equivalent [3], [8]. Consequently, the measurement resulting from pulse-echo characterizations such as in [1], [2] is the autoconvolution of the one-way impulse response. Hence we propose to retrieve the one-way impulse response from such a measurement in conjunction with a newly developed de-autoconvolution algorithm, although other algorithms are available as well [9–12]. More specifically, we measure the pulse-echo response of a flat plate reflector, which is especially time-efficient for large linear arrays. The flat reflector only needs to be aligned once after which all the measurements can be obtained for all array elements without any adjustments or alignments between measurements.

In Section II, we will first describe the measurement setup and the de-autoconvolution algorithm. In Section III we show the experimental results of the proposed technique, after which we provide a conclusion and discussion in Sections IV and V.

II. METHODS

A. Characterization procedure

Here we propose a simple calibration procedure to obtain autoconvolved measurements of the one-way impulse response. However, we would like to point out that the de-autoconvolution algorithm described in the next section should work with any measurement procedure that obtains an autoconvolved impulse response.

We suggest to place a flat plate reflector in front of the ultrasound transducer, parallel to the transducer surface, and measure the pulse-echo response after exciting the transducer by a delta-pulse. Since flat reflectors act as an acoustic mirror, the reflection does not change the temporal ultrasound waveforms before reflecting. Assuming the experiment takes place in a homogeneous medium, and assuming delta-pulse excitation, the sampled pulse-echo signal $x[n]$ can be modelled as: $x[n] = h_t[n] * g_t[n] * g_r[n] * h_r[n]$, where $h_t[n]$ and $h_r[n]$ are the electro-mechanical transmit and receive impulse responses of the transducer, respectively, and “*” denotes temporal convolution. The signals $g_t[n]$ and $g_r[n]$ represent the Green’s functions for the wavefield propagation to and from the flat reflector (see e.g. [13–15] for convolutive ultrasound models). In the described setup, it is straightforward to see that $g_t[n] = g_r[n]$. Assuming self-reciprocal transducers, $h_t[n] = h_r[n]$, and consequently $x[n]$ can be expressed as $x[n] = h[n] * g[n] * g[n] * h[n]$. This measurement can be de-autoconvolved to obtain the forward field $h[n] * g[n]$. If the flat reflector is placed appropriately, $g[n] = \delta[n - \tau]$, where τ depends on the distance to the flat reflector, such that $x[n] = h[n - \tau] * h[n - \tau]$. The time-shifted one-way impulse response $h[n - \tau]$ can then be obtained using de-autoconvolution.

For this setup it is important to align the flat reflector parallel to the transducer surface and place it at an appropriate distance to avoid sensor diffraction effects, such that $g[n] = \delta[n - \tau]$. If one is interested in the pulse-echo response of every sensor in a linear array, the flat reflector can simply be properly aligned with the array surface, after which the pulse-echo signal of each array sensor is measured one by one. This way, proper reflector alignment only needs to be done once for a large collection of sensors.

B. De-autoconvolution algorithm

Suppose we have measured the pulse-echo signal $x[n] = h[n] * h[n]$, and that the time-of-arrival delay τ is included in $h[n]$ from now on. Since linear convolution in the time-domain equals multiplication in the frequency domain, the magnitude spectrum of $h[n]$ can be obtained by taking any square root of each frequency of the Fourier transform of $x[n]$. Unfortunately, this results in a large set of solutions since all combinations of both the positive and negative square root are valid.

If the Discrete Fourier Transform (DFT) is used instead of a Discrete Time Fourier Transform (DTFT), multiplication in the DFT domain equals *circular* convolution in the time domain. Fortunately, linear autoconvolution can be expressed as a circular autoconvolution by zero-padding $h[n]$ until it has length $2N - 1$ samples, where N is the original length of $h[n]$, followed by a circular autoconvolution. Denote the set of solutions formed by taking any combination of positive and negative roots of the DFT of $x[n]$ by C . Any of these solutions solve the circular autoconvolution problem, whereas we are only interested in the linear version of the problem. It is easy to see that any solution to the linear problem is located in the set C as well. Moreover, they can be identified since such solutions must be a zero-padded signal. That is, a solution $\hat{h}[n]$ such that $\hat{h}[n] = 0$ for $n = N + 1, N + 2, \dots, 2N - 1$.

is a solution to the linear autoconvolution problem. Hence, to find a solution to the linear problem we look for solutions with this structure in the set C , which is equivalent to finding a solution for which the energy of the ‘tail’ of the estimated signal is zero. Next, we show how finding such a solution can be cast as a semi-definite programming problem.

Let the matrix $\bar{\mathbf{F}} \in \mathbb{C}^{(N-1) \times (2N-1)}$ denote the lower half of the inverse DFT matrix, corresponding to the tail of the signal in the time domain if right-multiplied with a DFT signal. Represent $x[n]$ by the vector $\mathbf{x} \in \mathbb{R}^{2N-1}$, and define the vector $\tilde{\mathbf{x}}$ as the point-wise positive square root of the DFT of \mathbf{x} . Finally, let \mathbf{p} be a $(2N - 1)$ -dimensional vector with components equal to ± 1 , corresponding to selecting either the positive or negative root in $\tilde{\mathbf{x}}$. To minimize the tail energy, we solve the following problem:

$$\min_{\mathbf{p}} \mathbf{p}^H \text{diag}(\tilde{\mathbf{x}})^H \bar{\mathbf{F}}^H \bar{\mathbf{F}} \text{diag}(\tilde{\mathbf{x}}) \mathbf{p} \quad \text{s.t.} \quad p_i \in \{-1, 1\}, \quad (1)$$

where H represents the conjugate transpose, and $\text{diag}(\tilde{\mathbf{x}})$ represents the square matrix where the diagonal is equal to $\tilde{\mathbf{x}}$. Once \mathbf{p} is obtained, it can be pointwise multiplied with $\tilde{\mathbf{x}}$ to obtain the estimate for $h[n]$ in the DFT domain. Problem (1) is a binary quadratic optimization problem which is known to be NP-complete. One way to still obtain a solution that (hopefully) comes close to the optimal solution is by means of semidefinite relaxation. After defining $\mathbf{P} = \mathbf{p}\mathbf{p}^H$ and $\mathbf{Q} = \text{diag}(\tilde{\mathbf{x}})^H \bar{\mathbf{F}}^H \bar{\mathbf{F}} \text{diag}(\tilde{\mathbf{x}})$, we have that $\mathbf{p}^H \mathbf{Q} \mathbf{p} = \text{Tr}(\mathbf{p}^H \mathbf{Q} \mathbf{p}) = \text{Tr}(\mathbf{Q} \mathbf{p} \mathbf{p}^H) = \text{Tr}(\mathbf{Q} \mathbf{P})$. Taking into account that \mathbf{p} in (1) is real, problem (1) can then be equivalently written as

$$\begin{aligned} \min_{\mathbf{P} \in \mathbb{R}^{(2N-1) \times (2N-1)}} \quad & \text{Tr}(\mathbf{Q} \mathbf{P}) \\ \text{s.t.} \quad & [\mathbf{P}]_{ii} = 1, \\ & \mathbf{P} \succeq 0, \\ & \text{rank}(\mathbf{P}) = 1 \end{aligned} \quad (2)$$

If this problem is relaxed by removing the rank constraint, the resulting convex problem can be solved by the following semi-definite program:

$$\begin{aligned} \min_{\mathbf{P} \in \mathbb{R}^{(2N-1) \times (2N-1)}} \quad & \text{Tr}(\mathbf{Q} \mathbf{P}) \\ \text{s.t.} \quad & [\mathbf{P}]_{ii} = 1, \\ & \mathbf{P} \succeq 0 \end{aligned} \quad (3)$$

To obtain a solution that still comes close to a rank one solution, we use random hyperplane rounding as in [16].

III. RESULTS

A. Numerical simulations

We first demonstrate the effectiveness of the de-autoconvolution on arbitrary signals. We generated 1000 random zero-mean unit-variance white Gaussian signals $h[n]$, and autoconvolved them to obtain $x[n]$. In all cases we were able to exactly reconstruct the original signal $h[n]$. Next, we simulated noisy measurements with additive zero-mean white Gaussian noise $v[n]$, $x[n] = h[n] * h[n] + v[n]$, and using an SNR of 20 dB. In this case, the average correlation between the estimated and true impulse response is 0.85 on average, with standard

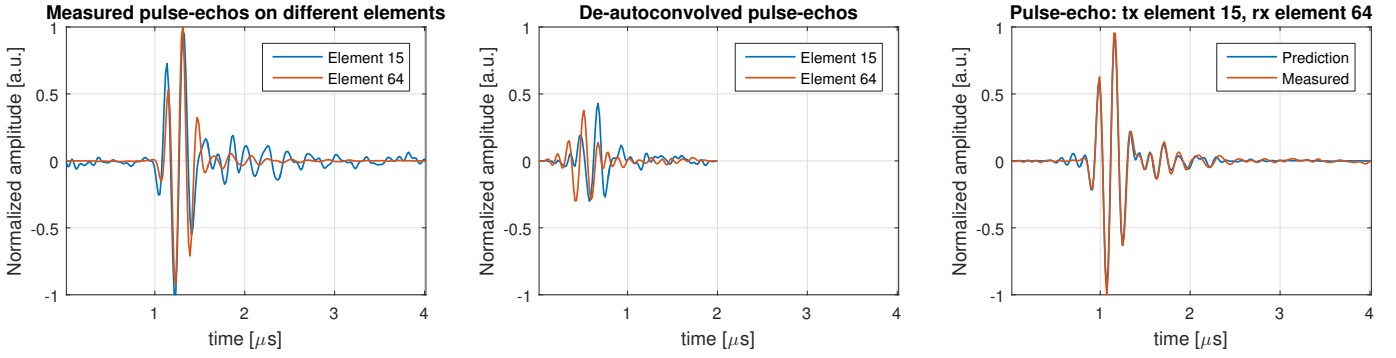


Fig. 1: Example to illustrate estimation and validation of the one-way impulse responses, including propagation effects, for two different elements, based on pulse-echo measurements of a thin wire in water. Left: the measured *pulse-echo* responses for two different elements. Each signal is obtained by transmitting and receiving on the same element. The signals are significantly different. Centre: the estimated *one-way* impulse responses obtained using de-autoconvolution. Right: comparison of the estimated and measured pulse-echo when transmitting on element 15 and receiving on element 64. The predicted echo is obtained by convolving the estimated one-way impulse responses. Note: we aligned pulses with different time-of-arrivals so they are more easily compared, and only plot from the moment echoes arrive (time-scales are not absolute).

deviation 0.23. Of these simulations, 77% of the estimates has a correlation higher than 0.9. Exact conditions for recovery and noise robustness for this particular algorithm are a topic of future research.

B. Experiment: flat reflector in water

We placed a flat perspex reflector parallel to a 128 element linear array (Philips/ATL L7-4) at a distance of 25 mm, coupled to an open ultrasound system (Vantage 256 channels, Verasonics Inc. Kirkland WA USA). To avoid diffraction effects, the reflector was placed as parallel as possible to the array. The elements were excited one by one by a delta-like pulse to obtain the autoconvolved impulse-responses for each element, and were then de-autoconvolved with the proposed algorithm to obtain $\hat{h}[n]$. To validate the results we subsequently measured pulse-echo responses from a perspex flat reflector using different transmit and receive elements. We then compared those measurements to the convolution of the estimated one-way impulse responses of those elements. The comparison is quantified by computing the normalized correlation between the measurement and the estimate. Figure 2 shows the average normalized correlation value between all elements in the array with the same inter-distance between transmit and receive elements. For larger inter-channel distance, the angle of arrival and departure becomes larger, and the role of diffractive effects become non-negligible. The Green's function $g[n]$ can no longer be considered to be a shifted delta-pulse, and we are comparing the estimate $\hat{h}_t[n] * \hat{h}_r[n]$ to the measured signal $h_t[n] * g_r[n] * g_r[n] * h_r[n]$. This is apparent from the downward trend in Fig. 2.

C. Experiment: thin wire in water

Instead of estimating the impulse response $h[n]$, we now consider estimating $h[n] * g[n]$ for a single point in space. To this end, we placed a thin wire in water, and kept its position fixed relative to the centre of the array, at a depth of 25 mm. By transmitting and receiving on the same channel, we basically measure the autoconvolution of $h[n] * g[n]$, which describes both the transducer transfer function as well as the propagation effects. Since the wire is in a fixed position, $g[n]$ is different for each element due to a different incident angle. After estimating $h[n] * g[n]$, we can predict the pulse-echo signal when transmitting and receiving on different elements. Figure 1 shows some example measurements and estimates. Figure 3 shows the radio frequency signals (RF) before and after de-autoconvolution. After de-autoconvolution, the RF resembles an RF where the wire itself is the ultrasound source. We further compare the normalized correlation coefficient similarly to the experiments with the flat reflector. The results are shown in Fig. 2. In this case, diffractive effects are included in the term $g[n]$, so that the estimation performance does not decrease as the inter-channel distance increases.

IV. DISCUSSION

An inherent property of the proposed method is that it estimates the transfer function of the entire system involved

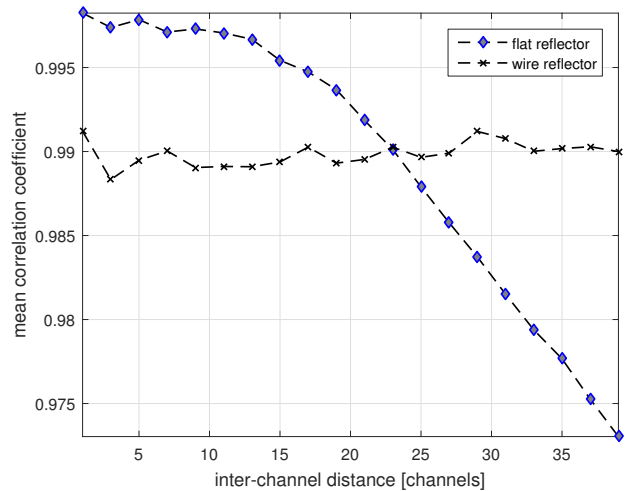


Fig. 2: Mean correlation between measured pulse-echo impulse response and the convolution of the estimated one-way impulse responses of those elements. The horizontal axis indicates the distance between transmit and receive elements.

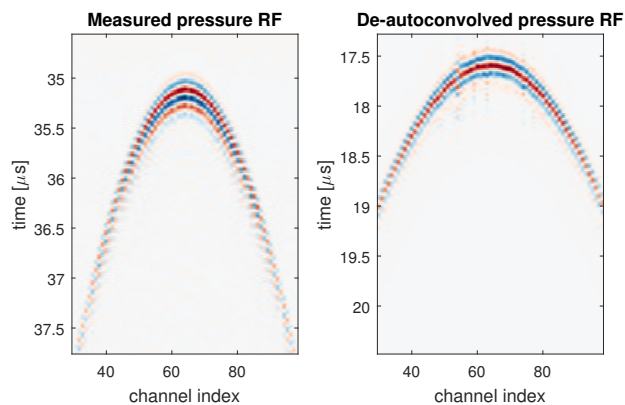


Fig. 3: Left: measured RF consisting of doing a pulse-echo measurement with the same transmit and receive channels. Right: de-autoconvolved RF of the left panel. The time-of-arrivals are two times shorter, and the pulse-lengths have decreased.

in the measurement, including the effect of the cable transfer functions, for example. As a result, simulations are more accurate by including all these effects and system electronics that are complicated to model [17]. An essential condition for successful estimation using our method is the self-reciprocity of the ultrasound transducer. This condition can be violated if different equipment or signal paths are used on transmit or receive, prohibiting successful calibration.

Some non-causal oscillation is visible at the beginning of the predicted signal in Fig. 3 in the right panel. This can be caused by an incorrect selection of the sign of the root in the vector \mathbf{p} , resulting in an incorrect phase for the corresponding frequency component.

Topics for future research are noise robustness, conditions for convergence of the semi-definite relaxation, and the use of additional constraints such as the limited bandwidth of a transducer, which is currently not exploited and could improve noise-robustness. The proposed de-autoconvolution algorithm should be compared to other de-autoconvolution methods in an ultrasound characterization context. The de-autoconvolution technique could potentially be used for estimating transmission signals for time-reversal focusing [18]. Finally, the fact that de-autoconvolution shortens the RF pulse-lengths could be interesting in the context of image reconstruction.

V. CONCLUSION

We outlined a de-autoconvolution algorithm and proposed a calibration procedure to use this algorithm for estimating the one-way impulse response of self-reciprocal ultrasound transducers. After careful alignment of a flat reflector, all characterization measurements for the entire array are rapidly obtained. We provide simulations to demonstrate the performance of the algorithm for random Gaussian signals with a white power spectral density. We show experimental results to illustrate its effectiveness with an array where the one-way impulse response is different for each element. The predicted pulse-echo signals based on the estimated one-way impulse responses correlate well with experimental measurements. We discussed the validity of the self-reciprocity condition and provided an outlook on future research topics.

REFERENCES

- [1] T. L. Szabo, B. Ü. Karbeyaz, R. O. Cleveland, and E. L. Miller, "Determining the pulse-echo electromechanical characteristic of a transducer using flat plates and point targets," *the Journal of the Acoustical Society of America*, vol. 116, no. 1, pp. 90–96, 2004.
- [2] T. Gehrke, F. Cheikhrouhou, and H. M. Overhoff, "Derivation of the impulse response of ultrasonic transducers by experimental system identification," in *Ultrasonics Symposium, 2005 IEEE*, vol. 1. IEEE, 2005, pp. 349–352.
- [3] K. Beissner, "Free-field reciprocity calibration in the transition range between near field and far field," *Acta Acustica united with Acustica*, vol. 46, no. 2, pp. 162–167, 1980.
- [4] W. Shou, S. Duan, P. He, R. Xia, and D. Qiari, "Calibration of a focusing transducer and miniature hydrophone as well as acoustic power measurement based on free-field reciprocity in a spherically focused wave field," *IEEE transactions on ultrasonics, ferroelectrics, and frequency control*, vol. 53, no. 3, pp. 564–570, 2006.
- [5] A. L. Lopez-Sanchez and L. W. Schmerr, "Determination of an ultrasonic transducer's sensitivity and impedance in a pulse-echo setup," *IEEE transactions on ultrasonics, ferroelectrics, and frequency control*, vol. 53, no. 11, 2006.
- [6] S. Zhang, C. M. Kube, Y. Song, and X. Li, "A self-reciprocity calibration method for broadband focused transducers," *The Journal of the Acoustical Society of America*, vol. 140, no. 3, pp. EL236–EL241, 2016.
- [7] K. Brendel and G. Ludwig, "Calibration of ultrasonic standard probe transducers," *Acta Acustica united with Acustica*, vol. 36, no. 3, pp. 203–208, 1976.
- [8] L. L. Foldy and H. Primakoff, "A general theory of passive linear electroacoustic transducers and the electroacoustic reciprocity theorem. i," *The journal of the acoustical society of America*, vol. 17, no. 2, pp. 109–120, 1945.
- [9] R. Gorenflo and B. Hofmann, "On autoconvolution and regularization," *Inverse Problems*, vol. 10, no. 2, p. 353, 1994.
- [10] K. Choi and A. D. Lanterman, "An iterative deautoconvolution algorithm for nonnegative functions," *Inverse problems*, vol. 21, no. 3, p. 981, 2005.
- [11] Z. Dai and P. K. Lamm, "Local regularization for the nonlinear inverse autoconvolution problem," *SIAM Journal on Numerical Analysis*, vol. 46, no. 2, pp. 832–868, 2008.
- [12] S. Bürger and J. Flemming, "Deautoconvolution: A new decomposition approach versus tigr and local regularization," *Journal of Inverse and Ill-posed Problems*, vol. 23, no. 3, pp. 231–243, 2015.
- [13] P. R. Stepanishen, "Pulsed transmit/receive response of ultrasonic piezoelectric transducers," *The Journal of the Acoustical Society of America*, vol. 69, no. 6, pp. 1815–1827, 1981.
- [14] J. A. Jensen and N. B. Svendsen, "Calculation of pressure fields from arbitrarily shaped, apodized, and excited ultrasound transducers," *IEEE transactions on ultrasonics, ferroelectrics, and frequency control*, vol. 39, no. 2, pp. 262–267, 1992.
- [15] A. Lhémy, "Impulse-response method to predict echo-responses from targets of complex geometry. part i: Theory," *The Journal of the Acoustical Society of America*, vol. 90, no. 5, pp. 2799–2807, 1991.
- [16] M. X. Goemans and D. P. Williamson, "Improved approximation algorithms for maximum cut and satisfiability problems using semidefinite programming," *Journal of the ACM (JACM)*, vol. 42, no. 6, pp. 1115–1145, 1995.
- [17] T. Kim, S. Shin, H. Lee, H. Lee, H. Kim, E. Shin, and S. Kim, "Matlab/simulink pulse-echo ultrasound system simulator based on experimentally validated models," *IEEE transactions on ultrasonics, ferroelectrics, and frequency control*, vol. 63, no. 2, pp. 290–302, 2016.
- [18] M. Fink, "Time reversal of ultrasonic fields. i. basic principles," *IEEE transactions on ultrasonics, ferroelectrics, and frequency control*, vol. 39, no. 5, pp. 555–566, 1992.